Available online at www.sciencedirect.com
SCIENCE DIRECT®
Journal of Molecular Graphics and Modelling 23 (2005) 389–394
Journal of Molecular Graphics and Modelling
www.elsevier.com/locate/JMGM

Structure analysis of the protein transduction domain of human Period1 and its mutant analogs

Xiao Lin Yang[a], Jun Xie[b], Bo Niu[b], Xiao Nian Hu[a], Yang Gao[a], Qian Xiang[a], Yue Hong Zhang[b], Yong Guo[c], Zheng Guo Zhang[a,*]

[a]*Department of Biomedical Engineering, Institute of Basic Medical Sciences, Peking Union Medical College, Chinese Academy of Medical Sciences, Beijing 100005, China*
[b]*Department of Biochemistry, Shanxi Medical University, Taiyuan, Shanxi Province, China*
[c]*Department of Neuroscience, Aventis Pharmaceuticals Inc., Bridgewater, NJ 08807, USA*

Received 7 November 2003; received in revised form 11 November 2004; accepted 15 November 2004
Available online 18 December 2004

Abstract

Human Period1 (hPer1) has been proved to be able to translocate into cells in a protein transduction manner. The segment of amino acids 830–845 of hPer1 is its protein transduction domain (PTD). In order to explore the membrane penetrating mechanism of hPer1-PTD and the physico-chemical properties necessary in the process, Ala scanning mutation method was used to investigate the variation in the peptide internalization. To further investigate the related physico-chemical requirements, the three dimensional structures of hPer1-PTD and its mutant analogs were simulated by Rosetta method. The electrostatic potentials and energies of these structures were calculated using the Delphi algorithm to solve Poisson–Boltzman equation. The hydrophobicity was assessed by the percentage of the nonpolar area in SAS (solvent accessible surface (SAS)). It has been proved that the Arg836 was the key residue for peptide internalization. When this Arg mutated into Ala, the peptide could not cross the membrane. The large enough area with positive charge was the decisive factor for hPer1-PTD. The alpha-helical structure seemed to play an assistant role so as to enable the positive charge connected in spatial arrangement.

Keywords: Human Period1; Protein transduction domain; α-Helix; Electrostatic; Hydrophobility

1. Introduction

In 1988, Green and Loewenstein [1] and Frankel and Pabo [2] independently reported that the HIV-1 Tat protein can cross the plasma membrane. This internalization is independent of receptor or transmitter, but depends on concentration. The Tat protein can enter almost all target cells at 37 and 4 °C. Its internalization is different from uptake by the classical endocytosis pathway. From then on, several other proteins, such as HSV-VP22 [3] Drosophila Antennapedia homeoprotein (ANTP) [4], and human Period1 (hPer1) [5] have been found to be able to traverse the cell membrane in a similar manner. The functional domain for protein transduction was mapped to a 10–30 amino acid segment (protein transduction domain (PTD)), which is rich in positively charged amino acids Arg and Lys. The PTDs have been proved to be able to deliver a large range of molecular cargo, such as oligonucleotides, peptides, full-length protein and even 40 nm superaramagnetic iron nanoparticles [6–8] into cells and tissues, and even across the blood–brain barrier [9]. Thus, protein tranduction has opened up new possibilities in biomedical research.

The precise mechanism of transduction mediated by PTDs has been the subject of much debate. Derossi et al. [10] and Wadia and Dowdy [11] have suggested different models for the transduction of ANTP and Tat. There are both three-step models. The first step is initiated by the interaction of positively charged PTD and the negatively charged outer membrane of the cell. The negatively charged proteoglycans

* Corresponding author. Tel.: +86 10 65296436; fax: +86 10 65137536.
E-mail address: z.g.zhang@ieee.org (Z.G. Zhang).

1093-3263/$ – see front matter © 2004 Elsevier Inc. All rights reserved.
doi:10.1016/j.jmgm.2004.11.008

on the surface of cells, such as heparan sulfate [12,13] and polysialic acid [14], seem to play an important role in the process of Tat and ANTP transduction. The second step is how PTDs cross the membrane. Although this step is still largely unknown, recent progress has been made in mechanism of Tat-PTD mediated transduction across the cell membrane. Dowdy and co-workers suggested that Tat-PTD internalization was performed by lipid raft-dependent macropinocytosis [15]. The third step involves series events in order to release the cargo molecule and keep it active intracellularly. By now, the positive net charge, α-helical structure and hydrophobicity are thought to be related factors in PTDs internalization, but their roles seem to be various in different PTDs [16–19]. Systematic studies need to be carried out to define their functions in the peptide internalization.

Human Period1 is a recently identified new protein that has the ability to traverse cell membrane. It has been proved that its PTD is located in the segment between amino acids 830 and 845 of hPer1 [5]. We carried out an Ala-Scan experiment in which each amino-acid of hPer1-PTD was substituted by an alanine residue. The analogs were fluorescently labeled to assess the transduction ability of hPer1-PTD and its mutant analogs in order to identify that the pivotal residue(s) in hPer1-PTD transduction process. Then the conformational and physico-chemical factors were analyzed based on the modeled 3D structures of these peptides, combined with their internalization ability.

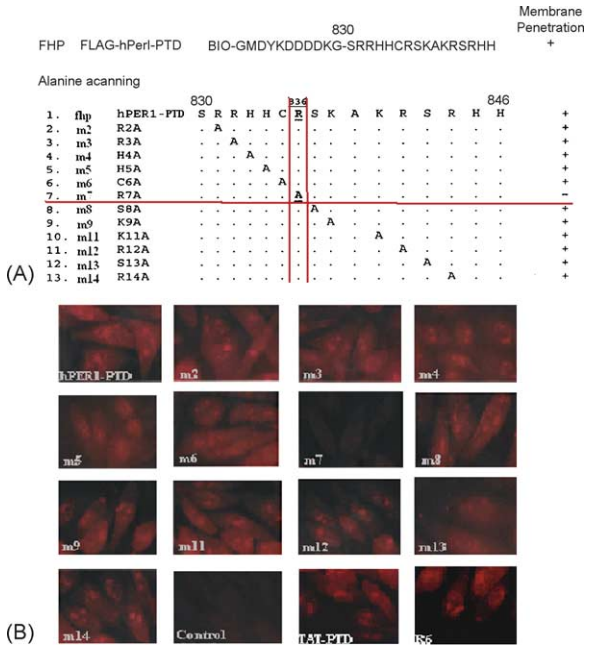

Fig. 1. Transduction of hPer1-PTD and its Alanine scanning mutant analogs. (A) Sequences of Flag-hPer1-PTD (fhp) and its mutant analogs. The 3D structures were modeled based on the sequences mentioned above. (B) Confocal microscopy of biotinylated hPer1-PTDs and its Alanine scanning mutant analogs transduction in CHO cells. Control peptide was from hPer1 N-terminal amino acid residues 486–500. R6 and Tat-PTD is positive control peptides. The result shows that only m7 cannot cross the membrane.

2. Methods

2.1. Peptides and peptide internalization

The sequences of hPer1-PTD and its mutant analogs were listed in the panel A of Fig. 1. These peptides were synthesized, purified and biotinylated by Biosynthesis Inc. (Lewisville, TX). Peptides were dissolved in DMSO and diluted with PBS.

CHO cells were cultured on overchips in Dulbecco's modified Eagle's medium supplemented with 10% fetal calf serum, penicillin 50 U/ml, streptomycin 50 μg/ml, and 4 mM L-glutamine at 37 °C with 5% CO_2. The culture medium was changed in every 3 days.

For peptide internalization, CHO cells were plated into two-well Lab-Tek coverclips (Nalge Nunc Inc., Naperville, IL) at a density of 2×10^5 cells/well and cultured overnight at 37 °C. The CHO cells were incubated with the peptides dissolved in the medium at the concentration of 1 μM for 10 min. Subsequently, cells were rinsed three times with PBS at room temperature and fixed in 4% (v/v) formaldehyde in PBS at room temperature for 20 min. The cell were washed three times in PBS, and incubated with labeled Streptavidin Alexa-594 (red, 2 μg/ml) (Molecular Probes), 1:400 diluted in 0.2% Tween 20, 2% BSA in PBS for 1 h at room temperature followed by 2×5 min washes with PBS and 20 min wash with 0.3% Triton X-100 in PBS. The sub-cellular localization of the fluorescence was analyzed with an Olympus microscope. Confocal images were taken on a Zeiss confocal laser scan microscope.

2.2. Structure modeling

The sequences that have been used in the structure modeling are shown in panel A of Fig. 1. The backbone of the 3D structure of the PTD of hPer1 and its mutant analog was determined using the Rosetta method [20,21]. The prediction server returned five models of the backbone. These structures were completed by searching side chain rotamer conformations in the Biopolymer module of InsightII (Accelrys Inc. USA). Then we used Profile-3D [22] to assess the quality of these structures. The structure with the highest score was chosen. The obtained structures were subjected to energy minimization under CFF91 [23] force field in order to optimize their conformations, using the Discover module of InsightII. First, the steepest descent minimization was performed on the model until the root mean square derivative was less than 10 kcal/mol/Å. Second, conjugate gradient minimization was carried out until the root mean square derivative was less than 0.01 kcal/mol/Å. In order to evaluate the quality of the modeled

structure, Profile-3D and PROCHECK [24,25] was used for validation.

2.3. Calculation of electrostatic potentials by Delphi

The electrostatic potentials of these structures were calculated in three different environments: solution (physical condition), vacuum and simulated lipid membrane. The peptides were placed into a 65 × 65 × 65 three-dimensional cubical grid. The grid resolution was 0.833 Å. In the solvent, we employed the internal and external dielectric constant values of 2 and 80; solvent and ionic probe radii of 1.4 and 2 Å, respectively, and 0.145 M (physiological) ionic strength. Full Coulombic boundary condition was applied. Non-linear option was toggled on, and the number of iterations was set to a value of 500. Other parameters were recommended default values. In vacuum and simulated lipid membrane condition, the external dielectric constants were 1 and 8, respectively. In these two environments, the ionic strength was 0. Other parameters were the same as those for the solution condition.

The input file of Delphi is the coordinate of the atoms of the protein. We chose the PDB format file without atomic charges and used the DelPhi library charge files for the calculations. In such a choice, it may be necessary to rescale charges as would be required in any polarized model. The output files recorded the energy value and potential map. The electrostatic potential distribution was mapped onto the molecular Connolly surface.

2.4. Calculation of solvent accessible surface (SAS)

We used homology module in InsightII to calculate the solvent accessible surface as defined by Lee and Richards [26], total surface area, fractional surface area, and polar/nonpolar surface area. The radius of the probe was set at 1.4 Å.

3. Result

3.1. Arginine 836 was essential for hPer1-PTD

Based on the fact that the PTD of hPer1 lies between amino acids 830 and 845, we sought to determine if there were key residues within hPer1-PTD that were important for its membrane penetrating potential. We replaced each amino acid separately in hPer1-PTD with alanine (Fig. 1), and assayed for the ability of these mutated peptides to penetrate living cells relative to the wild-type hPer1-PTD. As shown in Fig. 1, most of the single alanine substitutions had very little effect on membrane penetrating capability as compared with wild type hPer1-PTD except changing Arg836 to Ala. This substitution, R836A reduced the detectable cytological signal to that observed for the negative control peptides. This mutation significantly reduced the membrane penetrating properties of hPer1-PTD.

3.2. The structure of hPer1-PTD and its mutant analogs

The 3D structure models of hPer1-PTD and its mutant analogs are shown in Fig. 2. Profile-3D and PROCHECK analyses indicated that these 3D structures were reasonable one. And the structure of hPer1-PTD had been deposited in the PDB (1UL6).

Among the modeled structures, m3, m4, m5, m6, m7, m8, fhp, m12, m13, m14 (as listed in Fig. 1) had α-helix in its PTD functional segment (12–27). In addition m3, m4, m6, m8, m12 and m14 had a turn closely following the α-helix closely. This characteristic of the α-helix of hPer1-PTD is consistent with those of other proteins, which interact with lipid membranes, such as transducin [27] and bacterial toxin colicin A [28].

3.3. The electrostatic potentials of hPer1-PTD and its mutant analogs

As shown in Fig. 3, we can see a notable difference between the potential distributions of hPer1-PTD (fhp) and m7. In fhp, there was a large rectangle of positively charged region (blue) along the axis of its α-helix on one side, while no such polarized region was found on the opposite side. Relatively large positively charged regions could also be found in m3, m4, m5, m8 and m12 (data not shown). On the contrary, only small and separated polarized regions were found on the surface of m7, which was the only peptide that could not internalize protein cargo into the cell.

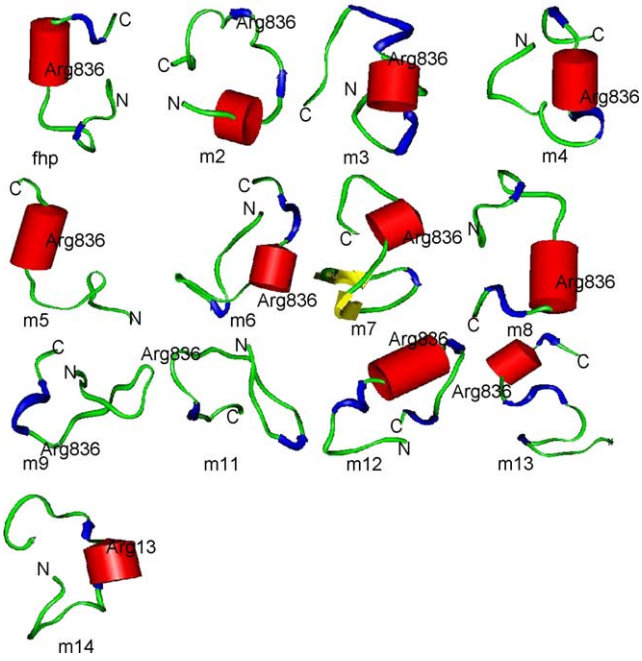

Fig. 2. Schematic structures of Flag-hPer1-PTD and its mutants. Red column represents the α-helix. In every structure, Arg836 (Ala) was labeled. M2, m8 and m9 did not form α-helixes in their PTD segment. In other structures, with the exception of m13, the Arg836 (Ala 836) is located in the α-helix. The structures were displayed using InsightII in SGI.

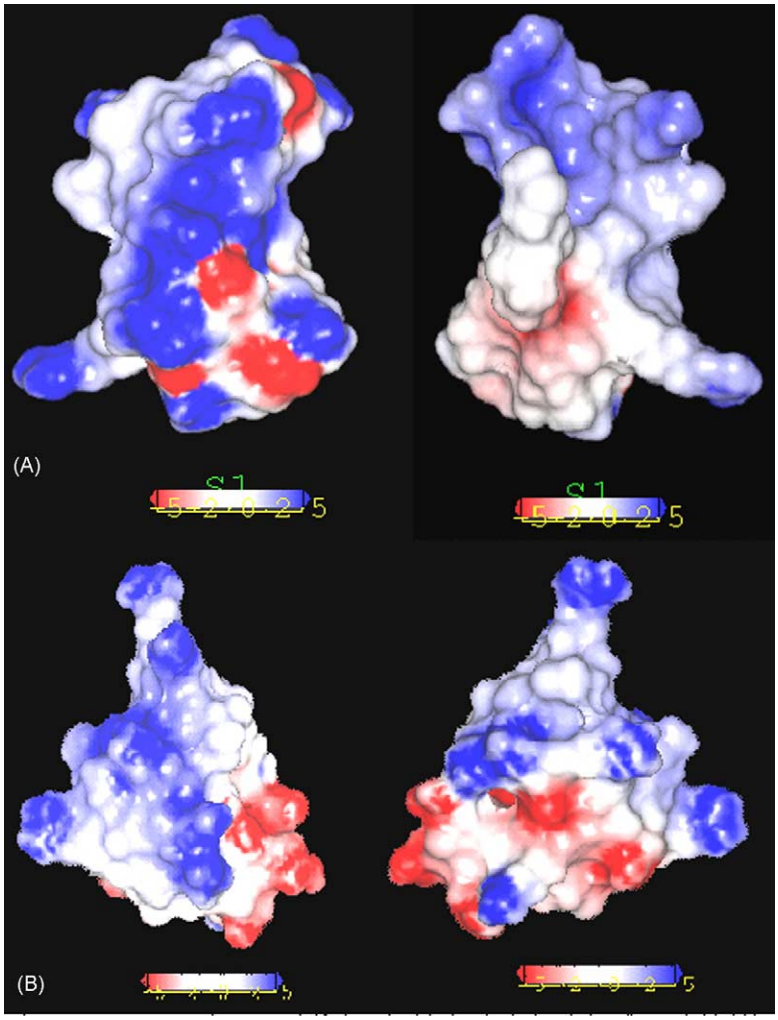

Fig. 3. The electrostatic potential of the surfaces of Flag-hPer1-PTD and m7 in solvent. Panels A and B display, respectively the electrostatic distribution of Flag-hPer1-PTD and m7 on two opposite sides of the molecule. The electrostatic potential is colored blue for positive and red for negative. The electrostatic potential distribution was calculated using Delphi, and visualized by InsightII in SGI.

The total plus grid electrostatic energy was calculated using Delphi. The electrostatic component of the salvation energy could be computed using two calculations with identical grid mappings and the same interior dielectric constants. The electrostatic energy of transfer from solvent to stimulated lipid membrane was calculated as follows:

$$\Delta G_{\mathrm{E}}(80,8) = G_{\mathrm{E}}(1,80) - G_{\mathrm{E}}(1,8)$$

Fig. 4 shows the calculated ΔG_{E} (80,8) of hPer1 and its mutant analogs. M7 had the largest value, which was 173.47 kcal/mol, while the values of other peptides between 90.75 kcal/mol (m9) and 130.82 kcal/mol (fhp). These results indicate that m7 must overcome the highest energy barrier from electrostatic forces.

3.4. Hydrophobic character of hPer1 and its mutant analogs

We have demonstrated that the percentage of SAS in the total surface area of a molecule had no significant difference among these peptides. The values ranged from 43.84% (m3) to 53.87% (m5) (data not shown). Comparing the percentage of nonpolar area in SAS, we found that the value for m7 was significantly lower than those of other molecules (Fig. 5).

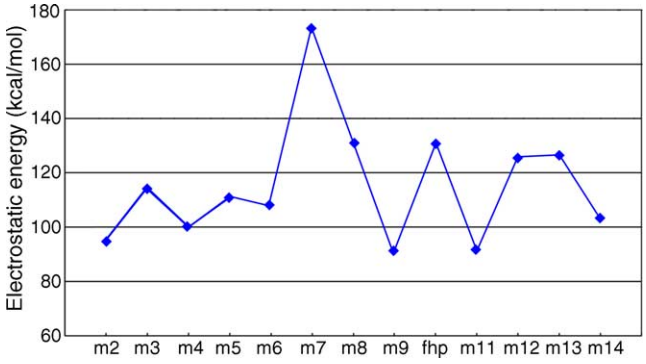

Fig. 4. The electrostatic energy of transfer from solvent to the stimulated lipid membrane. M7 was the only peptide that could not cross the cell membrane. It had the significantly higher energy value.

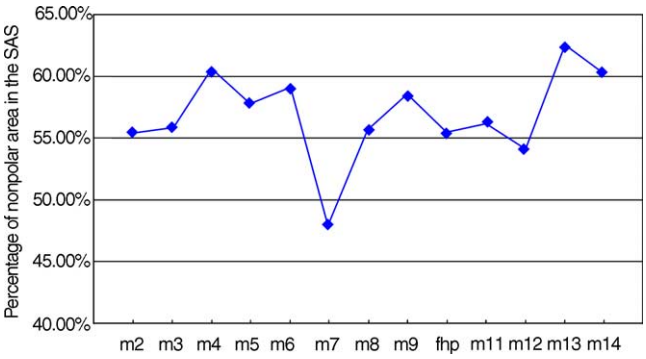

Fig. 5. The percentage of nonpolar area in the SAS of different mutants of hPer1. This figure indicates that the value of m7 is far smaller than other structures.

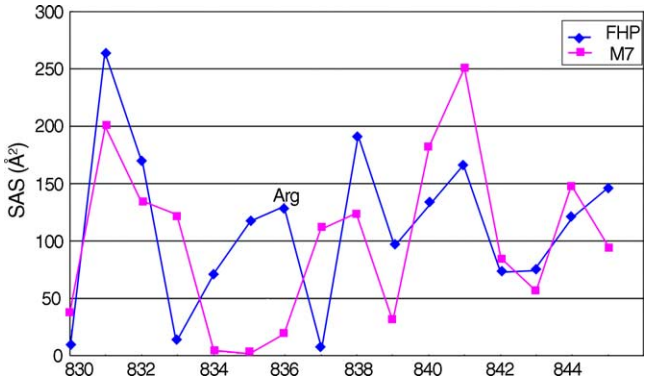

Fig. 6. The residue SASs (Å^2) of fhp and m7 When the Arg836 of fhp mutated to Ala, the SAS of other basic residues (R831, R832 and K838) in m7 turned smaller, but the SAS of S837 became larger.

This was an indication that m7 was more hydrophilic than the other peptides. We also compared the SAS of each residue. Fig. 6 shows the difference between m7 and fhp. With the mutation of R836A, the SAS of several other basic residues (R831, R832 and K838) turned smaller and the SAS of S837 became larger. Such changes also demonstrated that the positively charged region of m7 was small and could not be connected.

4. Discussion

Human Per1 is a component in the circadian clock and plays an important role in the regulation of daily oscillations. Recent study has been proved that the peptide segment 830–845 of hPer1 can cross the membrane as a PTD [5]. In this paper, we studied the sequence elements important for the hPer1-PTD internalization by using Ala-Scan mapping in which each amino acid was substituted by an alanine residue. The structures of these hPer1-PTD mutant analogs were predicted and analyzed to explore the conformational and physicochemical properties for cellular uptake of hPer1-PTD.

According to the result of cellular uptake experiment, only one mutant m7 (R836A) lost its penetrating ability among all ala mutant analogs. Such result indicated that the Arg played an important role in the hPer1-PTD cellular uptake and the relative position of Arg in different sequences also was related to their membrane penetrating function when their net positive charge was same. We, further, investigated how this mutation changed its structure and physicochemical properties based on modeled structures. In the 13-modeled structures, 10 of them have α-helical structure, including fhp and m7. For hPer1-PTD, it had an α-helix with positive charged region in one side of the helix as shown in Fig. 3. Such structural character coincided with several other PTDs. Tat-PTD [29], ANTP-PTD [30,31] and model amphipathic peptide I (MAP-I) [32,33] have been demonstrated to form α-helical structures and the basic residue gathered in one side of the helix. However, R6 (RRRRRR), an efficient PTD, had no evidence that it possessed the α-helical structure. Additionally, three mutant analogs of hPer1-PTD, which could cross the membrane, had no α-helix, Base on these results, we concluded that the large enough positive charged region was necessary for the internalization of PTD and that α-helical structure was favorable to the concentration of positive charge. The important reason for m7 lost the ability to cross the membrane was its small and dispersed positive charged region.

Another possible physicochemical factor related to cellular uptake is hydorphobicity. For MAP-1, the hydrophobic interaction between the amphipathic peptide with the outer layer of bilayers was thought to be required [32,34]. Although single residue mutation to improve the amphipathicity of Tat-PTD would increase the transduction efficiency of Tat-PTD [12], it has not been proved that hydrophobicity played an important role in membrane penetrating of Tat-PTD. Because the number of hydrophobic residues was limited in hPer1-PTD sequence, the hydrophobicity could not be a substantial factor to affect the membrane penetrating process. On the other hand, the hydropholicity of m7 is significantly low than other peptides. We think the mutation of R836A reduces the possibility of the interaction between the peptide and the membrane further.

5. Conclusion

Our study revealed that certain properties of hPer1 may be important for its penetrating function. First, Arg836 is the key residue for the membrane penetrating of hPer-PTD. Second, there should be large enough distribution region of its positive electrostatic potential for the interaction with the negatively charged membrane. This is the main property related to its membrane penetrating. The α-helical structure is an assistant factor for hPer1-PTD. The mutation of Arg836 to Ala made the peptide fail to cross the membrane

because of the lack of large enough region with positive charge and the decrease of hydrophobility.

Acknowledgement

We thank Prof. Hui Yuan Luo for his critical reading of the manuscript and helpful discussions.

Reference

[1] M. Green, P.M. Loewenstein, Autonomous functional domains of chemically synthesized human immunodeficiency virus tat transactivator protein, Cell 55 (1988) 1179–1188.
[2] A.D. Frankel, C.O. Pabo, Cellular uptake of the tat protein from human immunodeficiency virus, Cell 55 (1988) 1189–1193.
[3] A. Joliot, C. Pernelle, H. Deagostini-Bazin, A. Prochiantz, Antennapedia homeobox peptide regulates neural morphogenesis, Proc. Natl. Acad. Sci. U.S.A. 88 (1991) 1864–1868.
[4] G. Elliott, P. O'Hare, Intercellular trafficking and protein delivery by a herpesvirus structural protein, Cell 88 (1997) 223–233.
[5] Y. Guo, N.L. Cheng, X.X. Wang, Z.Z. Liu, J. Xie, hPer1-NLS: a novel protein transduction domain, J. Shanxi Med. Univ. 33 (2002) 197–198.
[6] L. Josephson, C.H. Tung, A. Moore, R. Weissleder, High-efficiency intracellular magnetic labeling with novel superparamagnetic-Tat peptide conjugates, Bioconjug. Chem. 10 (1999) 186–191.
[7] M. Lewin, N. Carlesso, C.H. Tung, X.W. Tang, D. Cory, D.T. Scadden, R. Weissleder, Tat peptide-derivatized magnetic nanoparticles allow in vivo tracking and recovery of progenitor cells, Nat. Biotechnol. 18 (2000) 410–414.
[8] C.H. Dodd, H.C. Hsu, W.J. Chu, P. Yang, H.G. Zhang, J.D. Mountz Jr., K. Zinn, J. Forder, L. Josephson, R. Weissleder, J.M. Mountz, J.D. Mountz, Normal T-cell response and in vivo magnetic resonance imaging of T cells loaded with HIV transactivator-peptide-derived superparamagnetic nanoparticles, J. Immunol. Methods 256 (2001) 89–105.
[9] S.R. Schwarze, A. Ho, A. Vocero-Akbani, S.F. Dowdy, In vivo protein transduction: delivery of a biologically active protein into the mouse, Science 285 (1999) 1569–1572.
[10] D. Derossi, G. Chassaing, A. Prochiantz, Trojan peptides: the penetratin system for intracellular delivery, Trends Cell Biol. 8 (1998) 84–87.
[11] J.S. Wadia, S.F. Dowdy, Protein transduction technology, Curr. Opin. Biotechnol. 13 (2002) 52–56.
[12] A. Ho, S.R. Schwarze, S.J. Mermelstein, G. Waksman, S.F. Dowdy, Synthetic protein transduction domains: enhanced transduction potential in vitro and in vivo, Cancer Res. 61 (2001) 474–477.
[13] D. Derossi, S. Calvet, A. Trembleau, A. Brunissen, G. Chassaing, A. Prochiantz, Cell internalization of the third helix of the Antennapedia homeodomain is receptor-independent, J. Biol. Chem. 271 (1996) 18188–18193.
[14] A.H. Joliot, A. Triller, M. Volovitch, C. Pernelle, A. Prochiantz, Alpha-2,8-Polysialic acid is the neuronal surface receptor of antennapedia homeobox peptide, New Biol. 3 (1991) 1121–1134.
[15] J.S. Wadia, R.V. Stan, S.F. Dowdy, Transducible TAT-HA fusogenic peptide enhances escape of TAT-fusion proteins after lipid raft macropinocytosis, Nat. Med. 10 (2004) 310–315.
[16] J.B. Rothbard, S. Garlington, Q. Lin, T. Kirschberg, E. Kreider, P.L. McGrane, P.A. Wender, P.A. Khavari, Conjugation of arginine oligomers to cyclosporin A facilitates topical delivery and inhibition of inflammation, Nat. Med. 6 (2000) 1253–1257.
[17] S. Futaki, T. Suzuki, W. Ohashi, T. Yagami, S. Tanaka, K. Ueda, Y. Sugiura, Arginine-rich peptides. An abundant source of membrane-permeable peptides having potential as carriers for intracellular protein delivery, J. Biol. Chem. 276 (2001) 5836–5840.
[18] G. Drin, M. Mazel, P. Clair, D. Mathieu, M. Kaczorek, J. Temsamani, Physico-chemical requirements for cellular uptake of pAntp peptide. Role of lipid-binding affinity, Eur. J. Biochem. 268 (2001) 1304–1314.
[19] A. Ziegler, J. Seelig, Interaction of the protein transduction domain of HIV-1 TAT with heparan sulfate: binding mechanism and thermodynamic parameters, Biophys. J. 86 (2004) 254–263.
[20] C.A. Rohl, D. Baker, De novo determination of protein backbone structure from residual dipolar couplings using Rosetta, J. Am. Chem. Soc. 124 (2002) 2723–2729.
[21] P.M. Bowers, C.E. Strauss, D. Baker, De novo protein structure determination using sparse NMR data, J. Biomol. NMR 18 (2000) 311–318.
[22] R. Luthy, J.U. Bowie, D. Eisenberg, Assessment of protein models with three-dimensional profiles, Nature 356 (1992) 83–85.
[23] B.M. Pettitt, M. Karplus, The potential of mean force surface for the alanine dipeptide in aqueous solution: a theoretical approach, Chem. Phys. Lett. 121 (1985) 194–201.
[24] A.L. Morris, M.W. MacArthur, E.G. Hutchinson, J.M. Thornton, Stereochemical quality of protein structure coordinates, Proteins 12 (1992) 345–364.
[25] R.A. Laskowski, M.W. MacArthur, D.S. Moss, J.M. Thornton, PROCHECK: a program to check the stereochemical quality of protein structures, J. Appl. Cryst. 26 (1993) 283–291.
[26] B. Lee, F.M. Richards, The interpretation of protein structures: estimation of static accessibility, J. Mol. Biol. 55 (1971) 379–400.
[27] D. Murray, S. McLaughlin, B. Honig, The role of electrostatic interactions in the regulation of the membrane association of G protein beta gamma heterodimers, J. Biol. Chem. 276 (2001) 45153–45159.
[28] J.H. Lakey, M.W. Parker, J.M. Gonzalez-Manas, D. Duche, G. Vriend, D. Baty, F. Pattus, The role of electrostatic charge in the membrane insertion of colicin A. Calculation and mutation, Eur. J. Biochem. 220 (1994) 155–163.
[29] P. Ruzza, A. Calderan, A. Guiotto, A. Osler, G. Borin, Tat cell-penetrating peptide has the characteristics of a poly(proline) II helix in aqueous solution and in SDS micelles, J. Pept. Sci. 10 (2004) 423–426.
[30] M. Lindberg, A. Graslund, The position of the cell penetrating peptide penetratin in SDS micelles determined by NMR, FEBS Lett. 497 (2001) 39–44.
[31] M. Magzoub, L.E. Eriksson, A. Graslund, Comparison of the interaction, positioning, structure induction and membrane perturbation of cell-penetrating peptides and non-translocating variants with phospholipid vesicles, Biophys. Chem. 103 (2003) 271–288.
[32] A. Scheller, J. Oehlke, B. Wiesner, M. Dathe, E. Krause, M. Beyermann, M. Melzig, M. Bienert, Structural requirements for cellular uptake of alpha-helical amphipathic peptides, J. Pept. Sci. 5 (1999) 185–194.
[33] J. Fernandez-Carneado, M.J. Kogan, S. Pujals, E. Giralt, Amphipathic peptides and drug delivery, Biopolymers 76 (2004) 196–203.
[34] J. Oehlke, A. Scheller, B. Wiesner, E. Krause, M. Beyermann, E. Klauschenz, M. Melzig, M. Bienert, Cellular uptake of an alpha-helical amphipathic model peptide with the potential to deliver polar compounds into the cell interior non-endocytically, Biochim. Biophys. Acta 1414 (1998) 127–139.